Novel atrazine-binding biomimetics inspired to the D1 protein from the photosystem II of Chlamydomonas reinhardtii

Amina Antonacci, Fabrizio Lo Celso, Giampaolo Barone, Pietro Calandra, Jörg Grunenberg, Maria Moccia, Emanuela Gatto, Maria Teresa Giardi, Viviana Scognamiglio

PII: S0141-8130(20)33753-3

DOI: https://doi.org/10.1016/j.ijbiomac.2020.07.010

Reference: BIOMAC 16058

To appear in: *International Journal of Biological Macromolecules*

Received date: 13 May 2020

Revised date: 2 July 2020

Accepted date: 2 July 2020

Please cite this article as: A. Antonacci, F.L. Celso, G. Barone, et al., Novel atrazine-binding biomimetics inspired to the D1 protein from the photosystem II of Chlamydomonas reinhardtii, *International Journal of Biological Macromolecules* (2020), https://doi.org/10.1016/j.ijbiomac.2020.07.010

Novel atrazine-binding biomimetics inspired to the D1 protein from the Photosystem II of *Chlamydomonas reinhardtii*

Amina Antonacci[1], Fabrizio Lo Celso[2,3], Giampaolo Barone[4], Pietro Calandra[5], Jörg Grunenberg[6], Maria Moccia[1], Emanuela Gatto[7], Maria Teresa Giardi[1,8], Viviana Scognamiglio[1]*

Amina Antonacci[1] and Fabrizio Lo Celso[2] equally contributed

[1] IC-CNR, Institute of Crystallography, National Research Council, Via Salaria km 29.300, 00015 Monterotondo, Rome, Italy.
[2] University of Palermo, Department of Physics and Chemistry, Viale delle Scienze Ed. 17
[3] Institute of Structure of Matter, National Research Council, Laboratorio Liquidi Ionici, Rome, Italy
[4] University of Palermo, Department STEBICEF, Viale delle Scienze Ed. 17
[5] ISMN-CNR, Institute of Nanostructured Materials, National Research Council, Via Salaria km 29.300, 00015, Monterotondo, Italy
[6] Institute of Organic Chemistry, Technische Universität Braunschweig, Braunschweig, Germany
[7] University of Rome "Tor Vergata", Department of Chemical Sciences and Technologies, 00133 Rome (Italy)
[8] Biosensor Srl, Via Olmetti 44, Formello, Italy

Abstract

Biomimetic design represents an emerging field for improving knowledge of natural molecules, as well as to project novel artificial tools with specific functions for biosensing. Effective strategies have been exploited to design artificial bioreceptors, taking inspiration from complex supramolecular assemblies. Among them, size-minimization strategy sounds promising to provide bioreceptors with tuned sensitivity, stability, and selectivity, through the *ad hoc* manipulation of chemical species at the molecular scale. Herein, a novel biomimetic peptide enabling herbicide binding was designed bioinspired to the D1 protein of the Photosystem II of the green alga *Chlamydomonas reinhardtii*. The D1 protein portion corresponding to the Q_B plastoquinone binding niche is capable of interacting with photosynthetic herbicides. A 50-*mer* peptide in the region of D1 protein from the residue 211 to 280 was designed *in silico*, and molecular dynamic simulations were performed alone and in complex with atrazine. An equilibrated structure was obtained with a stable pocked for atrazine binding by three H-bonds with SER222, ASN247, and HIS272 residues. Computational data were confirmed by fluorescence spectroscopy and circular dichroism on the peptide obtained by automated synthesis. Atrazine binding at nanomolar concentrations was followed by fluorescence spectroscopy, highlighting peptide suitability for optical sensing of herbicides at safety limits.

Keywords: artificial peptides, rational design, atrazine sensing

**Corresponding author*
Viviana Scognamiglio
Institute of Crystallography - National Research Council
Department of Chemical Sciences and Materials Technologies
Via Salaria km 29.300 - 00015 Monterotondo Scalo, Rome, Italy
viviana.scognamiglio@ic.cnr.it

1. Introduction

In the last decades, synthetic biology and biomimetic chemistry demonstrated huge potential to handle living matters by re-designing complex biological systems or their sub-components, with the aim to improve knowledge on biological mechanisms, as well as to furnish novel advantageous functions. In sensing field, for example, these multidisciplinary technologies allow for the design of powerful tuneable analytical tools able to respond to external *stimuli*, with customised properties in terms of sensitivity, selectivity, and stability, among others [1]. To realize that, the convergence of different technologies is required, including structural chemistry and rational design, to provide novel biological recognition elements for sensing applications, taking inspiration from complex supramolecular assemblies present in living organisms, whose effectiveness is the result of millennia of natural selection.

Due to the complex structure derived from the hierarchical organization of chemical species (e.g. polypeptides folded to form proteins) the overall property/function is often the result of a wide scenario of interactions from steric effects to polar-polar, Van deer Waals and dispersion interactions, as well as directional H-bonds, leading to emerging properties which cannot be usually traced back to short-range or single-molecule characteristics. In this framework, therefore, the key-point is the comprehension of the essential factor giving the desired functions: the successive size-minimization strategy getting rid of the unnecessary part of the complex structure renders the production of the biomimetic tool affordable. In this context, computer modelling can help in understanding the different roles of the various share of the overall chemical structure in order to better identify and select the essential fragments. However, due to the complex nature of the system and the high number of atoms involved, a detailed and accurate description, which could give trustful indications, is still a challenge.

Herein, we present the design of novel artificial biomimetic peptides through a rational size-minimization of the pivotal D1 protein from the green photosynthetic alga *Chlamydomonas reinhardtii*. This protein, together with the D2 protein, constitutes the heterodimer core of Photosystem II (PSII). Many intrinsic features have made D1 protein one of the most investigated photosynthetic protein, in particular on aspects related to structure-function, gene, messenger, protein regulation, electron transport, reactive oxygen species, photo inhibition, stromal-granal translocations, reversible phosphorylation, specific proteases, and herbicide binding [2, 3]. Focusing on D1 protein capability to bind either plastoquinone or xenobiotics, several studies have demonstrated the competitive atrazine interaction with D1 protein, physically entering in the same site of plastoquinone Q_B, and hence hindering the natural redox cascade reactions in the

photosynthetic system. In this context, with the aim to produce customised bioreceptors for sensing applications with tailored analytical features in terms of selectivity and sensitivity, we describe an *in silico* strategy to design novel synthetic peptides as a result of *ad hoc* size minimization of the photosynthetic herbicide-binding niche of the D1 protein. We also took advantage of our previous work [4], which describes the design, synthesis, and characterisation of a particular segment of 70 amino acids in the D1 protein involved in the formation the D1-plastoquinone assembly [5], to design a shorter version of 50 amino acids. The effectiveness of this size minimization together with the preservation of the atrazine-recognition functionality shed light at a molecular base on the essential factors regulating the protein inhibition by xenobiotic poisons. Furthermore, the possibility to exploit synthetic peptides, compared to supramolecular complexes, can not only greatly improve the features of biosensors, in terms of cost, time, reproducibility, selectivity and stability, but also allow for simpler and lower-cost synthesis of smart bioreceptors. In fact, in the case of extracted reaction centres (RC) or photosystems (PSII), long and expensive laboratory procedures are required [6,7]. Moreover, once produced, such photosynthetic sub-components, e.g. D1 protein, are highly sensitive to ROS species being degraded in few minutes. Finally, D1 protein in particular is highly hydrophobic, thus hindering its use as bioreceptor in biosensor design. It could be exploited as soluble protein only if solved in high concentrated detergents [8]; however, in such solvents the protein loose the typical structure of the binding site, thus lowering its affinity towards the target herbicides. The stability of the reaction centres is also a concern, considering that extracted RCs are stable for 20 min at room temperature, 1 hour at 4 °C, and 1 month at -20 °C [9]. On the other hand, the exploitation of whole cells means more variables as biological systems, and these aspects should not be underestimated during the development of a biosensor [3]. For this reason, the simple and cost-effective synthesis of artificial bioreceptors inspired to natural macromolecules is gaining momentum. In this study, by computational modelling and automated synthesis, a wild type and two mutated 50-*mer* peptides were obtained and further characterised by circular dichroism and fluorescence spectroscopy, to provide deep insights on their structural and functional features as well as their interaction dynamics in response to atrazine.

2. Materials and methods

2.1 Computational details

Protein and peptide structures and complexes with atrazine were modelled through molecular docking calculations, using the Autodock Vina package [10]. Molecular dynamic simulations were performed using the GROMACS 5.1.1 package [11, 12]. Interactions were described using an all-atoms CHARMM27 force field [13, 14]. The simulations for the various systems were performed using a cubic box of NaCl 150 mM in explicit TIP3P water solution. Periodic boundary conditions were applied. Force field parameter files and initial configuration for the polypeptides were created by GROMACS utilities programs. Force field parameters for atrazine was taken from the ATB repository [15]. The equilibration procedure was done in several steps, starting from a NVT simulation at 300K with the polypeptides heavy atom positions restrained to equilibrate the solvent around it, followed by a NPT run at 300 K and pressure at 1 bar, for a 10 ns run. After the equilibration phase, the system was run for a total of 300 ns for a NVT production run; the trajectory was saved at a frequency of 10 ps to evaluate dynamical and structural properties. The simulations were always checked versus the root mean square displacement (RMSD) and the energy profile. During the production runs for the temperature coupling, we used a velocity rescaling thermostat [16] (with a time coupling constant of 0.1 ps), while for the pressure coupling, we used a Parrinello-Rahman barostat [17] (1 ps for the relaxation constant). The Leap-Frog algorithm with a 2-fs time step was used for integrating the equations of motion. Cut-offs for the Lennard-Jones and real space part of the Coulombic interactions were set to 10 Å. For the electrostatic interactions, the Particle Mesh Ewald (PME) summation method [18] was used, with an interpolation order of 4 and 0.16 nm of FFT grid spacing. Selected images and peptide manipulation were done using Maestro [19] and VMD [20, 21]. To quantify the binding strength of the peptide-atrazine complexes their equilibrium geometry of the peptide-atrazine complexes was further fully optimized by the empirical UFF force field [22], using the Gaussian 09 program package [23]. The relaxed force constants of atrazine-peptide bonds were evaluated by the COMPLIANCE software [24, 25], after performing a vibration frequency analysis on the optimized geometry, in the harmonic approximation.

2.2 Peptide synthesis

The peptides were produced by automated synthesis by Aurogene S.R.L. (Via dei Lucani, 51, 00185 Rome, Italy). The peptides were synthesized by liquid phase peptide synthesis (LPPS) and solid phase peptide synthesis (SPPS), and purified to obtain samples with > 95% of purity. The synthetic molecules were analyzed by MS/HPLC and sequence confirmation was performed.

2.3 Circular dichroism

Circular dichroism spectra were performed under a nitrogen flow on a J-1500 Spectropolarimeter (Jasco, Tokyo, Japan) equipped with the Neslab RTE-110 temperature-controlled liquid system (Neslab Instruments, Portsmouth, NH). Peptide solutions of about 5.7 μM in 1 mM NaPi buffer pH 7.0, were placed in sealed cuvettes with a 0.1 cm path length (Hellma, Mullheim, Germany), and spectra were measured between 270 and 195 nm with the following setup: bandwidth 1 nm, response 0.25 sec, speed 20 nm/min, sensitivity 20 mdeg, 8 accumulations, and step resolution 1 nm. All spectra were averaged 16 times and smoothed with the Spectropolarimeter System Software (Jasco). Before measurements, all samples were temperature equilibrated for 5 min. During the measurement the photomultiplier voltage never exceeded 600 V. The results were expressed in terms of the molar ellipticity.

2.4 Fluorescence spectroscopy

Fluorescence spectra were recorded in 1 mM NaPi buffer, pH 7.0 peptide solutions. Steady-state fluorescence measurements were performed on a F-8200 Spectrofluorometer (Jasco, Tokyo, Japan) with a cell temperature-controlled sample holder, equipped with the Neslab RTE-110 temperature-controlled liquid system (Neslab Instruments, Portsmouth, NH). Peptide fluorescence was excited at 280 nm, with emission and excitation slit width of 5 nm. Before measurements, all samples were temperature equilibrated for 5 min.

3. Results and discussion

3.1 Computational results

The primary structure of *C. reinhardtii* Photosystem II (PSII) D1/D2 proteins was taken from Rea et al. (2009), which was built using the crystal structure of *Thermosynechococcus elongatus* D1/D2 proteins as template (PDB code 2AXT), thanks to the high sequence homology between the two reaction centres (87% and 89% amino acid sequence identity, respectively) [26]. From this structure, a fragment of 70 residues, D1Pep70-WT, known to bind atrazine, was designed from the D1 chain [4]. In a first step, detailed docking simulation served to produce putative host-guest structures, which were used as starting structures for our in-depth MD simulations, in order to explore both static and dynamic aspects. As a result of this approach, the molecular docking provided various complexes established by D1Pep70-WT with atrazine, with different scorings. Among them, the three top-score configurations for the D1Pep-70-WT complex with atrazine were selected (Figure S1), and used as initial configurations for our MD simulations. The details of the procedure followed for MD is described in the experimental section. Due to our simulations at the equilibrium stage (300 ns run), only one of the above three configurations, specifically the number **2** of Figure S1 (Supplementary Materials), resulted in a tertiary structure where atrazine is well placed inside the pocket. The analysis performed in the last 50 ns of the MD simulations with the g-cluster tool, within the GROMACS package [27], showed that the most probable structure is the one reported in Figure 1A, where the interaction between the two portions occurs via the residues PHE255, PHE265, and ALA263. In details, two kinds of interactions are present: N-based H-bond which involve ALA263 and PHE255, and π-π stacking involving PHE255 and PHE265. It must be noticed that the residue PHE265 can interact in both ways and that all these interactions involve two different segments in the tertiary structure of the peptide chain. Nevertheless, due to the calculated relaxed force constants these interactions are negligible, being lower than 0.2 N/cm.

The diverse interactions and the cooperation between different peptide segments in atrazine stabilization suggest that eventual actions on the peptide sequence, aiming at reducing its length, must preserve the delicate equilibrium between interactions and the overall geometry. For this reason, a new fragment of 50 residues, D1Pep-50-WT, was created by substituting the amino acid residues from 224 to 245 with two glycine residues (Figure 1B). This choice allowed the cutting out of a quite linear chain of peptide not interacting with atrazine, simultaneously preserving distances and angles between residues 223 and 246. Thanks to the free rotation around σ-bonds, the short two-glycine segment backbone can be adapted to the two joint moieties sufficiently preserving, in

principle, the overall freedom in conformational dynamics. This cutting procedure was applied to the three equilibrium structures of D1Pep-70-WT/atrazine structures coming out from the MD simulations. Then, a new MD simulation was performed on each of the three D1Pep-50-WT/atrazine complexes. The result evidenced the equilibrated structure reported in Figure 2A. In this complex, atrazine is tightly inserted in the D1Pep-50-WT pocket and makes three H-bonds with residues SER222, ASN247 and HIS272. Noteworthy, atrazine seems to make a stronger binding with the shorter polypeptide than the longer one. In fact, as shown in Figure 2A, the molecule is closer to two alpha helices of polypeptide, in contrast to what observed in Figure 1A, in which atrazine interacts only with one branch of the polypeptide. However, similarly to the D1Pep70-WT/atrazine, the relaxed force constants of such interactions are lower than 0.2 N/cm also in D1Pep50-WT/atrazine complex. It can be concluded that the cutting out of the portion 224-245 would result to be effective, since it gives a shorter peptide which is, however, still able to bind atrazine. The primary structures of D1Pep70-WT and D1Pep-50-WT were reported in Table 1.

Molecular MD simulation shows that both bare peptide D1Pep-50-WT and its complex with atrazine possess similar structure. The two structures were superimposed in Figure 3A, showing that D1Pep-50-WT is slightly affected by the binding with the herbicide. From the experimental point of view, the chemically synthesized D1Pep-50-WT appears as a slight hydrophobic molecule soluble only in buffers containing DMSO (10% v/v). This, together with the calculated conformational minor changes of the peptide occurring when atrazine is bound, suggested a further action directed to the increase in peptide hydrophilicity.

For this reason, taking inspiration from a previous work [4] and considering the substitution of the peptide portion from residue 224 to 245 with 2 glycines, a new peptide (hereafter called as D1Pep-50-Mut) was designed on the basis of the previously reported sequence. In detail, 5 Phe residues (211, 260, 265, 273, and 274) were substituted with isosteric Tyr residues, and 3 Ala residues (213, 250, and 263) were substituted with more polar Ser residues. D1Pep-50-Mut is a 5639.26 Da molecule with a theoretical pI of 9.16 and an extinction coefficient at 280 nm measured in water equal to 17420 M^{-1} cm^{-1} (*Supporting Materials*), containing 7 tyrosine residues at positions 211, 246, 254, 260, 262, 265, 273, 274, a phenylalanine at position 255, and a tryptophan residue at position 278. The primary structures of D1Pep-50-Mut was reported in Table 1.

The typical MD procedure shows that the most probable structure of D1Pep-50-Mut is that depicted in Figure 2B. By perusal of the figure several clues can be derived:

i) the peptide structure is changed, as a consequence of the different primary structure of the peptide. This new structure is able to host atrazine in a position closer to its inner cavity.

ii) different residues now bind atrazine, in the specific SER264 and TYR265. Moreover, TYR265 was not present in D1Pep-50-WT, suggesting that its insertion evidently triggers the possibility for a strong peptide-atrazine bond, in this structure.

iii) the host-guest interactions can be characterized as strong H-bonds, with relaxed force constants of 10.0 and 17.4 N/cm, respectively [28].

Such values are more than one order of magnitude higher than those present in D1Pep-50-WT and in D1Pep70-WT. This also suggested that the change made in the peptide primary structure is crucial to stabilise the overall structure. These clues are confirmed by the calculation of the binding standard Gibbs free energy ($\Delta G°$) calculations: the insertion of atrazine in D1Pep-50-WT implies a $\Delta G°$ of -14 KJ mol^{-1}, whereas the value is decreased to -139 KJ mol^{-1} in the case of D1Pep50-Mut. The observed increase in the absolute value of the binding standard Gibbs free energy of a factor of ten, clearly confirms that changes made to prepare D1Pep50-Mut are crucial to increase its binding with atrazine. The derived binding constants are $3 \cdot 10^2$ and $\sim 10^{24}$ for D1Pep-50-WT / atrazine and D1Pep-50-Mut / atrazine complexes, respectively.

The strong interactions between D1Pep50-Mut and atrazine, as well as the atrazine binding through one portion of D1Pep50-Mut chain only (differently from D1Pep50-WT binding atrazine by two different portions of its chain), allows us to expect a marked peptide conformational change when the atrazine is inserted or taken out from the cavity. This would be an essential factor for producing a switch-type biosensor. This hypothesis is confirmed if the structures of the mutated peptide in the absence and in the presence of atrazine are compared. They were reported in Figure 3B, superimposed for better comparison. The final clue is therefore that D1Pep-50-WT structure is affected by the binding with the herbicide. The conformational change occurring upon atrazine binding is also evidenced by spectroscopic analysis. The overall result of MD simulation confirms that the change in the primary structure can end up in a quite hydrophilic peptide able to stably bind atrazine in its cavity and perform a conformational change consequent to its interaction.

3.2 Spectroscopic structural and functional characterisation

The structure and binding capability of the synthetic peptides D1Pep-50-WT and D1Pep-50-Mut were explored by circular dichroism (CD) and fluorescence spectroscopy (FS). The far-UV CD spectra of D1Pep-50-WT and D1Pep-50-Mut at 25 °C are reported in Figure 3A and B, respectively. CD spectra of D1Pep-50-WT shows a minimum at 228 nm, and it is similar to the one reported for helical peptides in aggregated conditions [29]. This could be ascribed to the low hydrophilicity of the molecule, which does not find a proper accommodation into a water solvent.

Moreover, the addition of atrazine is not able to provide any conformational change in the peptide structure as evidenced by the CD spectra. The CD profile of D1Pep-50-Mut is similar to the one of the parent peptide, but it has a lower intensity and the minimum is shifted to lower wavelengths (222 nm). This suggests that the D1Pep-50-Mut peptide is less aggregated than the wild type. Furthermore, atrazine addition induces a marked conformational change in the mutated peptide, as described by the CD spectra variations, which show an isodichroic point, suggesting equilibrium between two different conformations [30]. In accordance to CD spectra, the fluorescence emission spectrum of D1Pep-50-WT shows a double maximum, suggesting the presence of aggregation [31]. Both peptides show an intrinsic emission band of TRP278 centred at 345 nm, which indicates an indole ring quite exposed to the aqueous medium. Upon atrazine binding, the wild-type peptide provides increased fluorescence intensity, while the mutated one shows decreased fluorescence intensity, revealing the heterogeneity of the microenvironments of the fluorescent residues, which are spread in the two different structures.

In depth-fluorescence analyses were performed to shed light on the effect of herbicide binding on the structural stability of D1Pep-50-Mut. Variations of the D1Pep-50-Mut intrinsic fluorescence induced by physic denaturant agents (i.e. temperature), were determined in the absence and in the presence of atrazine. As shown in Figure 4A, the fluorescence melting curve of D1Pep-50-Mut decreases almost linearly in the range 25 - 95 °C. This transition exhibits a good cooperativity both in the absence and in the presence of 100 nM atrazine, giving a sigmoidal profile that fits with a two-state unfolding model and thus suggesting that structural change takes place in this temperature range. Interestingly, by fitting this curve, melting temperatures (T_M) of 30 and 45 °C were obtained in the absence and in the presence of 100 nM atrazine, respectively. This pattern indicates that atrazine induces a conformational change in the D1Pep-50-Mut structure stabilizing it, so that the fluorescent residues, directly (or indirectly) affected by its presence, display a cooperative transition at a higher temperature, as expected by a niche/site of a folded protein. In addition, with the rise of the temperature both a decrease of the fluorescence intensity and a red shift of the wavelength underline that the peptide has a folded structure which is subjected to an unfolding mechanism due to the temperature increase, indicating the displacement of the fluorescent residues to the solvent (Figure 4B).

In the framework of the design of novel bioreceptors for sensing applications, further characterization by fluorescence spectroscopy D1Pep-50-Mut was carried out to probe its binding ability for atrazine and, in particular, the effect of atrazine binding on peptide conformational properties. The binding ability of D1Pep-50-Mut towards atrazine was followed by fluorescence spectroscopy in a lower concentration range. Serial additions from 10 to 100 nM of atrazine were

supplied to D1Pep-50-Mut (5.7 µM), and the peptide intrinsic fluorescence emission intensity due to the fluorescent residues was recorded. The samples were excited at 280 nm and the emission was monitored in the 300 to 450 nm region. The fluorescence emission band decreases as the atrazine concentration increases. Corrections were made for dilution of the sample and for background signal from buffer. A linear response was obtained in the atrazine concentration range exploited allowing for the construction of a calibration curve using the linear regression reported by the equation y = 1(±0.005) - 0.005(±0.0013) x, with an $R^2 = 0.9983$ (Figure 4C). A detection limit of 4.8 nM was obtained (calculated as 3.3 × standard deviation of the regression line / slope).

4. Conclusions

The prime purpose of this work relies on the development of smarter bioreceptors for biosensor design, not only with custom-made analytical features, in terms of e.g. sensitivity, but also through simple and cost-effective procedures. In this context, the possibility to exploit artificial peptides, bioinspired to supramolecular complexes, can greatly improve the features of sensing systems, in terms of cost, time, reproducibility, selectivity, and sensitivity. Indeed, the laboratory procedures required for the production of natural photosynthetic sub-components, as reaction centres or photosystem extracts, can result highly laborious and expensive; on the other hand, the exploitation of whole cells, although very sensitive, entails higher biological variables, these aspects becoming extremely disadvantageous during the biosensor development [3].

In this scenario, novel biomimetic peptides for atrazine sensing were designed by *in silico* approach. In particular, molecular dynamic-based computer modelling showed that in the case of peptide D1Pep-50-Mut, the residues 211-280 portion of the Photosystem II (PSII) D1 protein from *C. reinhardtii* can be effectively subjected to size minimization (resides 226-245 substituted by two glycines) as well as to *ad hoc* mutations to improve their hydrophilicity, while preserving the final capability to bind atrazine. Despite the obvious changes in the interactions involved in atrazine binding, D1Pep-50-Mut showed to undergo structural changes upon target binding, making it a promising candidate for atrazine sensing. Experimentally, circular dichroism and fluorescence spectroscopy have self-consistently confirmed this possibility, highlighting also that the peptide possesses good thermal stability. Benefits of the peptide presented in this work include the reduced number of amino acids thus decreasing the complexity and costs of the peptide synthesis, the adequate water solubility, and the low detection limit (4.8 nM) towards atrazine, meeting the requirements of EU regulations (EU Directive 2013/39/EC). We believe that the accordance between the information experimentally derived and those foreseen by computer modelling is due

to the refined procedure adopted in our calculations, a resources-saving method, which can be tailored for *ad hoc* design of novel molecules in sensor applications and which could be of inspiration for future research.

Acknowledgement

This work was supported by *AdSWiM* Interreg Project Italy-Croatia 2019/2020 and *NanoSWS* project EraNetMed-RQ3-2016. M.T.G. was supported by POR FESR Campania "Good-Water" Project n. b63d18000150007.

Figure captions

Figure 1. A) Most frequent equilibrium structure of the complex between atrazine and D1Pep-70-WT. The 2D structure, highlighting the H-bond (in purple) and dispersion (in green) interactions, is also shown (inset). B) Picture showing the cut (orange to blue unstructured backbone) performed on D1Pep-70-WT to obtain the shorter D1Pep-50-WT model.

Table 1. Primary sequences of the obtained peptides. The amino acidic substitutions of the newly designed peptides are highlighted in yellow.

Figure 2. A) Most frequent equilibrium structure of the complex between atrazine and D1Pep-50-WT (left). The 2D structure, highlighting the H-bond (in purple) interactions, is also shown (right). The arrow points to the position where the cutting action was carried out. B) Most frequent equilibrium structure of the complex between D1Pep-50-Mut with atrazine (left). The 2D structure, highlighting the H-bond (in purple) interactions, is also shown (right). The molecular structures of D1Pep-50-WT and D1Pep-50-Mut are reported in electronic supporting materials as *pdb* files.

Figure 3. MD) Superimposed structures of the peptide-atrazine complex and the isolated peptide (in purple) with sequence D1Pep-50-WT (A) and sequence D1Pep-50-Mut (B). CD) Circular dichroism (centre) and FS) fluorescence spectroscopy (right) analysis for each peptide in the absence and in the presence of atrazine, with 100 nM as the first concentration (molar ratio peptide/atrazine 1:2). Arrows indicate the maximum atrazine concentration exploited (600 nM).

Figure 4. Temperature-induced conformational transitions of D1Pep-50-Mut (black curve) and its complex with atrazine (red curve) as changes in fluorescence intensity at 345 nm (A) and changes in wavelength (B). Calibration curve for atrazine with 100 nM as the maximum concentration (molar ratio peptide/atrazine 1:2) (C).

References

[1] V. Scognamiglio, A. Antonacci, M.D. Lambreva, S.C. Litescu, G. Rea, Synthetic biology and biomimetic chemistry as converging technologies fostering a new generation of smart biosensors. Biosens.Bioelectron. 74 (2015) 1076-1086. https://doi.org/10.1016/j.bios.2015.07.078.

[2] M. Edelman, A.K. Mattoo, D1-protein dynamics in photosystem II: the lingering enigma. Photosynth. Res. 98 (1-3) (2008) 609-620. https://doi.org/10.1007/s11120-008-9342-x.

[3] A. Antonacci, V. Scognamiglio, Biotechnological Advances in the Design of Algae-Based Biosensors. Trends Biotechnol. 38, 3, (2019) 334-347.
https://doi.org/10.1016/j.tibtech.2019.10.005.

[4] V. Scognamiglio, P., Stano, F. Polticelli, A. Antonacci, M.D. Lambreva, G. Pochetti, M.T. Giardi, G. Rea, Design and biophysical characterization of atrazine-sensing peptides mimicking the *Chlamydomonas reinhardtii* plastoquinone binding niche, PCCP 15 (2013) 13108-13115. https://doi.org/10.1039/C3CP51955D.

[5] J. Xiong, G. Jee, S. Subramaniam, Modeling of the D1/D2 proteins and cofactors of the photosystem II reaction center: Implications for herbicide and bicarbonate binding. Protein Science, 5 (10) (1996) 2054-2073. doi: 10.1002/pro.5560051012.

[6] Lupínková, L., & Komenda, J. (2004). Oxidative Modifications of the Photosystem II D1 Protein by Reactive Oxygen Species: From Isolated Protein to Cyanobacterial Cells. Photochemistry and Photobiology, 79(2), 152-162.

[7] Groß, A., Hashimoto, C., Sticht, H., & Eichler, J. (2016). Synthetic peptides as protein mimics. Frontiers in bioengineering and biotechnology, 3, 211.

[8] Khristin, M. S., & Simonova, N. B. (1998). Extraction and stability of the pigment-protein complexes of the photosystem 2 from membranes of the unicellular alga Dunaliella salina: effect of glycerol. Membrane & Cell Biology, 12(1), 57-66.

[9] Giardi, M. T., Marder, J. B., & Barber, J. (1988). Herbicide binding to the isolated photosystem II reaction centre. Biochimica et Biophysica Acta (BBA)-Bioenergetics, 934(1), 64-71.

[10] O. Trott, A.J. Olson, AutoDock Vina: Improving the speed and accuracy of docking with a new scoring function, efficient optimization, and multithreading, J. Comput. Chem. 31 (2010) 455–461. https://doi.org/10.1002/jcc.21334.

[11] B. Hess, C. Kutzner, D. Van Der Spoel, E. Lindahl, GROMACS 4: algorithms for highly efficient, load-balanced, and scalable molecular simulation. J. Chem. Theory Comput., 4(3), (2008), 435-447. https://doi.org/10.1021/ct700301q.

[12] D. Van Der Spoel, E. Lindahl, B. Hess, G. Groenhof, A.E. Mark, H.J. Berendsen, GROMACS: fast, flexible, and free. J. Comput. Chem, 26(16), (2005), 1701-1718. https://doi.org/10.1002/jcc.20291.

[13] N. Foloppe, A.D. MacKerell, Jr, All- atom empirical force field for nucleic acids: I. Parameter optimization based on small molecule and condensed phase macromolecular target data. J. Comput. Chem, 21(2), (2000), 86-104. https://doi.org/10.1002/(SICI)1096-987X(20000130)21:2%3C86::AID-JCC2%3E3.0.CO;2-G.

[14] A.D. MacKerell Jr, N.K. Banavali, All- atom empirical force field for nucleic acids: II. Application to molecular dynamics simulations of DNA and RNA in solution. J. Comput. Chem, 21(2), (2000), 105-120. https://doi.org/10.1002/(SICI)1096-987X(20000130)21:2%3C105::AID-JCC3%3E3.0.CO;2-P.

[15] A.K. Malde, L. Zuo, M. Breeze, M. Stroet, D. Poger, P.C. Nair, C. Oostenbrink, A.E. Mark, An Automated force field Topology Builder (ATB) and repository: version 1.0, J. Chem. Theory Comput., (2011), 7, 4026-4037. http://pubs.acs.org/doi/abs/10.1021/ct200196m.

[16] G. Bussi, D. Donadio, M. Parrinello, Canonical sampling through velocity rescaling. The Journal of chemical physics, 126(1), (2007), 014101. https://doi.org/10.1063/1.2408420.

[17] M. Parrinello, A. Rahman, Polymorphic transitions in single crystals: A new molecular dynamics method. Journal of chemical physics, 52(12), (1981), 7182-7190. https://doi.org/10.1063/1.328693.

[18] T. Darden, D. York, L Pedersen, The effect of long-range electrostatic interactions in simulations of macromolecular crystals–a comparison of the ewald and truncated list methods. J. Chem. Phys. 99, 10, (1993), 10089. http://dx.doi.org/10.1063/1.465608.

[19] Maestro, Schrödinger, LLC, New York, NY, 2018, version 11.6.010.

[20] W. Humphrey, A. Dalke, K. Schulten, VMD: visual molecular dynamics. Journal of molecular graphics, 14(1), (1996), 33-38.

[21] http://www.ks.uiuc.edu/Research/vmd/.

[22] A.K. Rappé, C.J. Casewit, K.S. Colwell, W.A. Goddard III, W.M Skiff, UFF, a full periodic table force field for molecular mechanics and molecular dynamics simulations. Journal of the American chemical society, 114(25), (1992), 10024-10035. https://doi.org/10.1021/ja00051a040.

[23] M. Frisch, G. Trucks, H. Schlegel, G. Scuseria, M. Robb, J. Cheeseman, G. Scalmani, V. Barone, B. Mennucci, G. Petersson, H. Nakatsuji, M. Caricato, X. Li, H. Hratchian, A. Izmaylov, J. Bloino, G. Zheng, J. Sonnenberg, M. Hada, M. Ehara, K. Toyota, R. Fukuda, J. Hasegawa, M. Ishida, T. Nakajima, Y. Honda, O. Kitao, H. Nakai, T. Vreven, J. Montgomery, J. Peralta, F. Ogliaro, M. Bearpark, J. Heyd, E. Brothers, K. Kudin, V. Staroverov, R. Kobayashi, J. Normand, K. Raghavachari, A. Rendell, J. Burant, S. Iyengar, J. Tomasi, M. Cossi, N. Rega, J. Millam, M. Klene, J. Knox, J. Cross, V. Bakken, C. Adamo, J. Jaramillo, R. Gomperts, R. Stratmann, O. Yazyev, A. Austin, R. Cammi, C. Pomelli, J. Ochterski, R. Martin, K. Morokuma, V. Zakrzewski, G. Voth, P. Salvador, J. Dannenberg, S. Dapprich, A. Daniels, Farkas, J. Foresman, J. Ortiz, J. Cioslowski, D. Fox, Gaussian 09, Revision A.1, Gaussian, Inc., Wallingford CT 2009. https://gaussian.com/glossary/g09/.

[24] K. Brandhorst, J. Grunenberg, Efficient computation of compliance matrices in redundant internal coordinates from Cartesian Hessians for nonstationary points. J. Chem. Phys. 132(18), (2010), 184101-7. https://doi.org/10.1063/1.3413528.

[25] K. Brandhorst, J. Grunenberg, How strong is it? The interpretation of force and compliance constants as bond strength descriptors. Chem. Soc. Rev. 37(8) (2008) 1558-1567. https://doi.org/10.1039/B717781J.

[26] G. Rea, F. Polticelli, A. Antonacci, V. Scognamiglio, P. Katiyar, S. A. Kulkarni, M.T. Giardi, Structure- based design of novel *Chlamydomonas reinhardtii* D1- D2 photosynthetic proteins for herbicide monitoring. Prot. Sci. 18(10), (2009) 2139-2151. https://doi.org/10.1002/pro.228.

[27] P. Söderhjelm, G. A. Tribello, M. Parrinello, Locating binding poses in protein-ligand systems using reconnaissance metadynamics. PNAS, 109(14), (2012) 5170-5175. https://doi.org/10.1073/pnas.1201940109.

[28] J. Grunenberg, Direct assessment of interresidue forces in Watson− Crick base pairs using theoretical compliance constants. Journal of the American Chemical Society, 126(50), (2004) 16310-16311. https://doi.org/10.1021/ja046282a

[29] E. Gatto, S. Kubitzky, M. Schriever, S. Cesaroni, C. Mazzuca, G. Marafon, M. De Zotti, Building Supramolecular DNA- Inspired Nanowires on Gold Surfaces: From 2D to 3D. Angew Chem Int Ed, 58(22), (2019) 7308-7312. https://doi.org/10.1002/anie.201901683.

[30] E. Gatto, M. E. Palleschi, B. Zangrilli, M. De Zotti, B. Di Napoli, A. Palleschi, M. Venanzi, The several facets of Trichogin GA IV: High affinity Tb (III) binding properties. A spectroscopic

and molecular dynamics simulation study. Pep Sci, 110(5), (2018) e24081. https://doi.org/10.1002/pep2.24081.

[31] L.L. Del Mercato, P. P. Pompa, G. Maruccio, A. Della Torre, S. Sabella, A.M. Tamburro R. Rinaldi, Charge transport and intrinsic fluorescence in amyloid-like fibrils. PNAS, 104(46), (2007) 18019-18024. https://doi.org/10.1073/pnas.0702843104.

Declaration of interests

The authors declare that they have no known competing financial interests or personal relationships that could have appeared to influence the work reported in this paper.

D1Pep70-WT	211-**FSAMHGSLVTSSLIRETTENESANEGYRFGQEEETYNIVAAHGYFGRLIFQYASFNNSRSLHFFLAAWPV**-280
D1Pep-50-WT	211-**FSAMHGSLVTSSLGG**-225 246-**YNIVAAHGYFGRLIFQYASFNNSRSLHFFLAAWPV**-280
D1Pep-50-Mut	211-**YSSMHGSLVTSSLGG**-225 246-**YNIVSAHGYFGRLIYQYSSYNNSRSLHYYLAAWPV**-280

Table 1

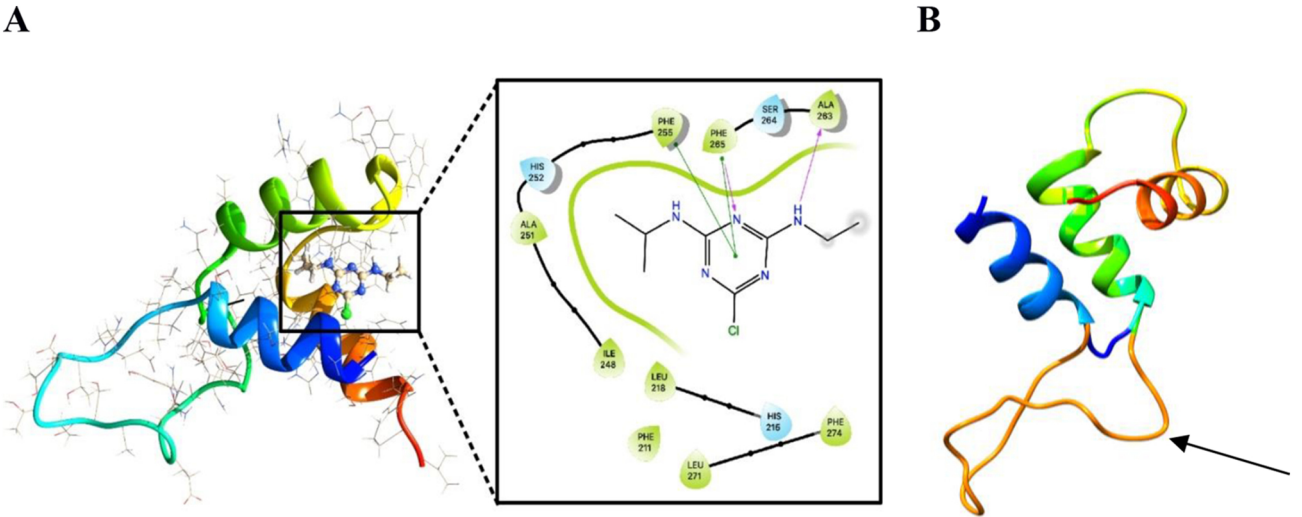
A
B
PHE 255
PHE 265
SER 264
ALA 283
HIS 252
ALA 251
ILE 248
LEU 218
HIS 216
PHE 274
PHE 211
LEU 271
H
N
N
N
N
H
Cl

Figure 1

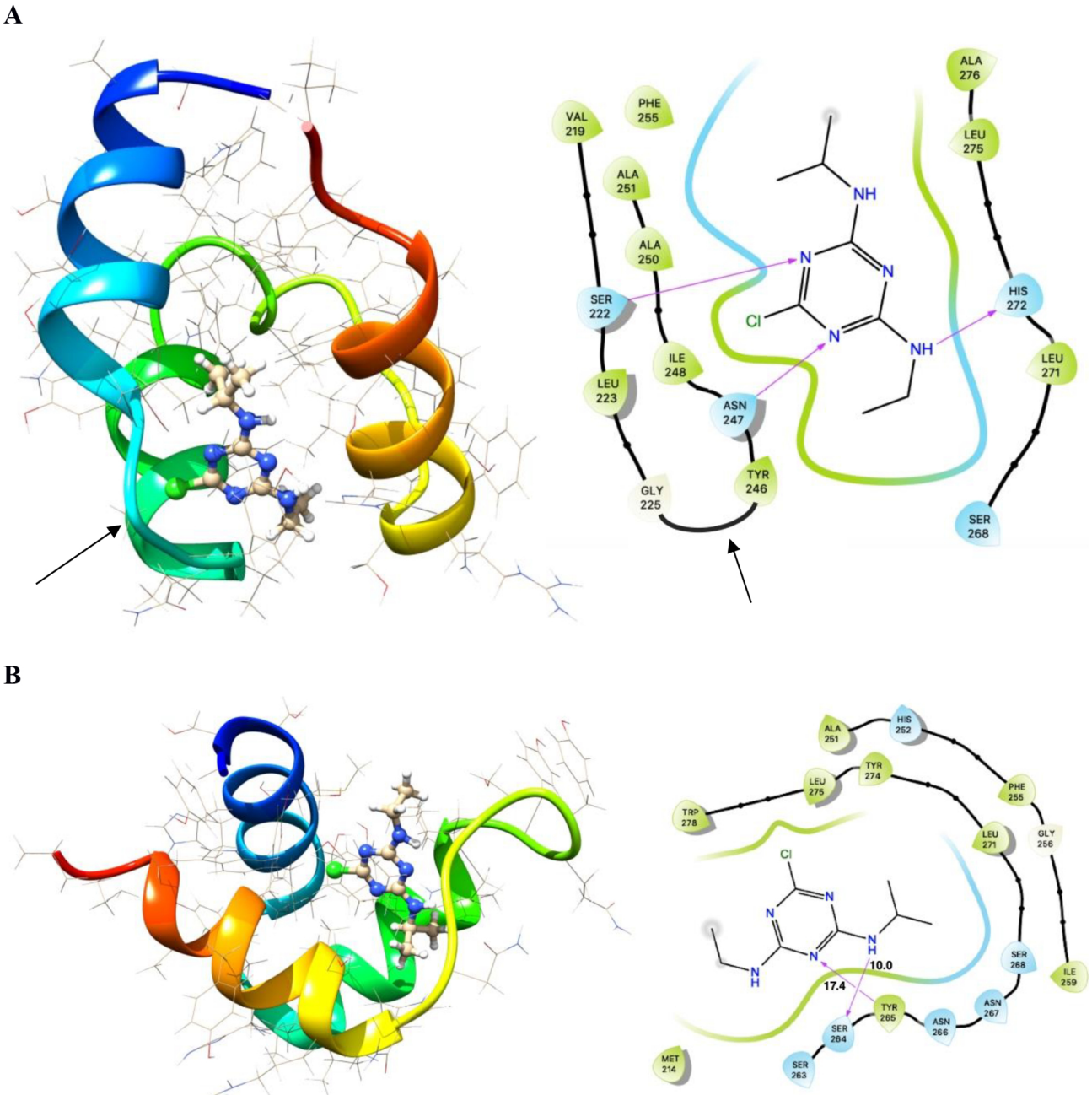
A
VAL 219
PHE 255
ALA 251
ALA 250
SER 222
ILE 248
LEU 223
ASN 247
GLY 225
TYR 246
ALA 276
LEU 275
HIS 272
LEU 271
SER 268
NH
N
N
Cl
N
NH
B
ALA 251
HIS 252
TYR 274
LEU 275
PHE 255
TRP 278
LEU 271
GLY 256
SER 268
ILE 259
ASN 267
TYR 265
ASN 266
SER 264
SER 263
MET 214
Cl
N
N
N
NH
NH
10.0
17.4

Figure 2

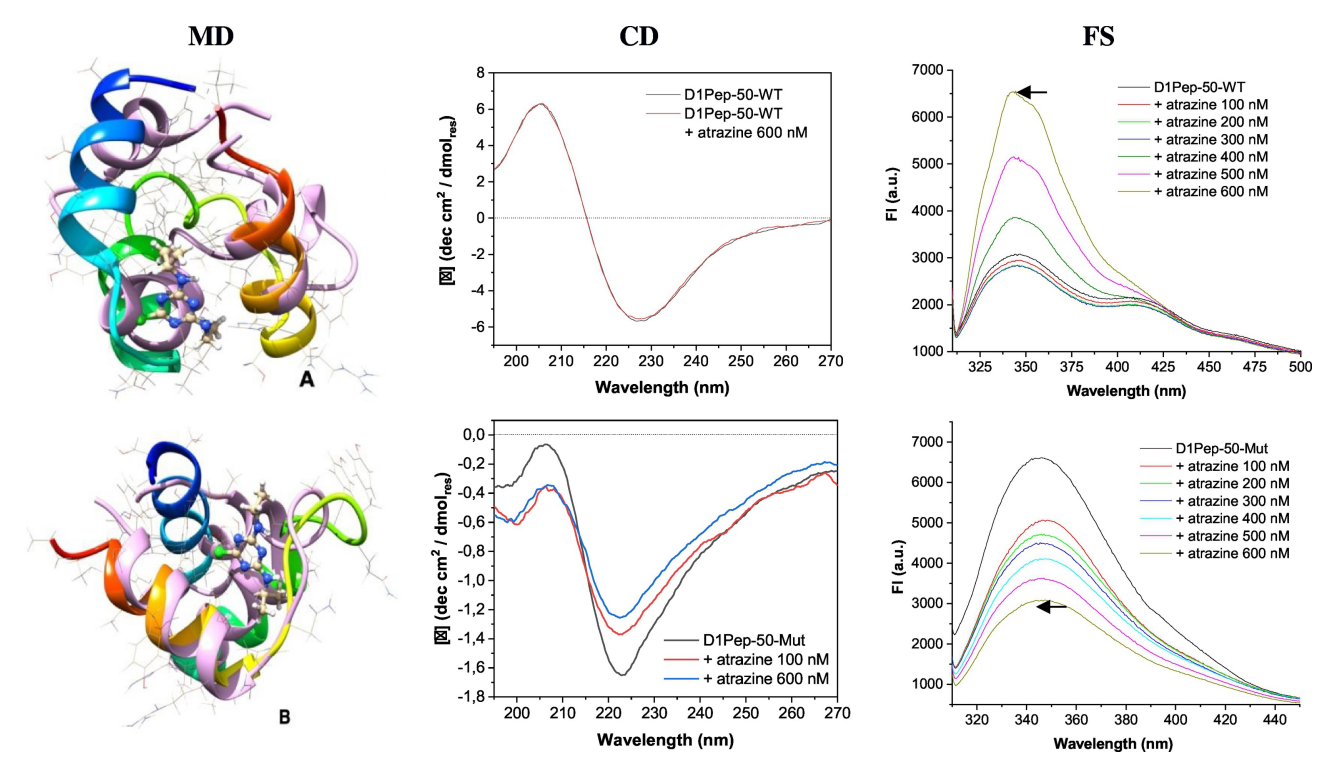
MD
CD
FS
A
B
D1Pep-50-WT
D1Pep-50-WT
+ atrazine 600 nM
[Θ] (dec cm² / dmol_res)
Wavelength (nm)
D1Pep-50-WT
+ atrazine 100 nM
+ atrazine 200 nM
+ atrazine 300 nM
+ atrazine 400 nM
+ atrazine 500 nM
+ atrazine 600 nM
FI (a.u.)
Wavelength (nm)
D1Pep-50-Mut
+ atrazine 100 nM
+ atrazine 600 nM
[Θ] (dec cm² / dmol_res)
Wavelength (nm)
D1Pep-50-Mut
+ atrazine 100 nM
+ atrazine 200 nM
+ atrazine 300 nM
+ atrazine 400 nM
+ atrazine 500 nM
+ atrazine 600 nM
FI (a.u.)
Wavelength (nm)

Figure 3

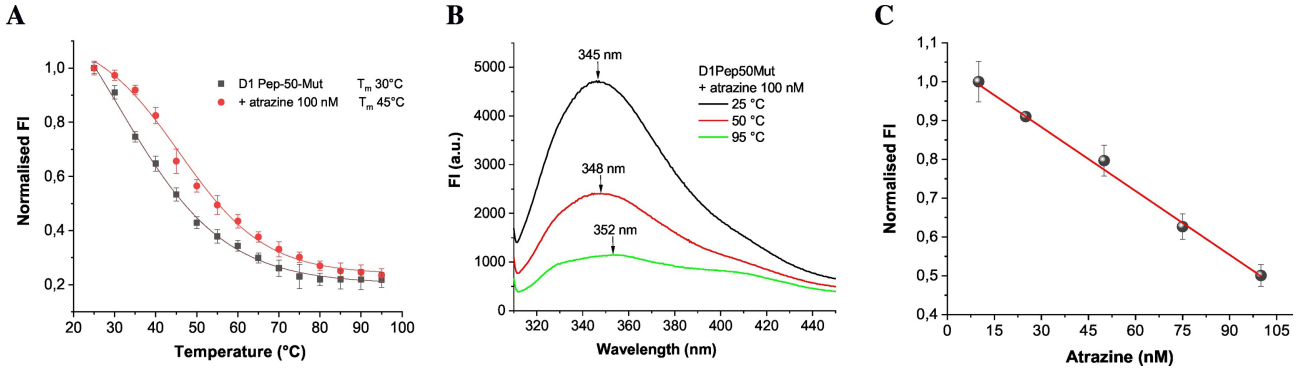
A
Normalised FI
D1 Pep-50-Mut
+ atrazine 100 nM
T_m 30°C
T_m 45°C
Temperature (°C)
B
FI (a.u.)
345 nm
348 nm
352 nm
D1Pep50Mut
+ atrazine 100 nM
25 °C
50 °C
95 °C
Wavelength (nm)
C
Normalised FI
Atrazine (nM)

Figure 4